Cytoplasmic MTOCs control spindle orientation for asymmetric cell division in plants

Ken Kosetsu[a,b,c], Takashi Murata[d,e], Moé Yamada[a], Momoko Nishina[a], Joanna Boruc[b,c], Mitsuyasu Hasebe[d,e], Daniël Van Damme[b,c,1], and Gohta Goshima[a,1]

[a]Division of Biological Science, Graduate School of Science, Nagoya University, Chikusa-ku, Nagoya 464-8602, Japan; [b]Department of Plant Biotechnology and Bioinformatics, Ghent University, 9052 Ghent, Belgium; [c]Center for Plant Systems Biology, VIB, 9052 Ghent, Belgium; [d]Division of Evolutionary Biology, National Institute for Basic Biology, Myodaiji-cho, Okazaki 444-8585, Japan; and [e]Department of Basic Biology, School of Life Science, The Graduate University for Advanced Studies (SOKENDAI), Myodaiji-cho, Okazaki 444-8585, Japan

Proper orientation of the cell division axis is critical for asymmetric cell divisions that underpin cell differentiation. In animals, centrosomes are the dominant microtubule organizing centers (MTOC) and play a pivotal role in axis determination by orienting the mitotic spindle. In land plants that lack centrosomes, a critical role of a microtubular ring structure, the preprophase band (PPB), has been observed in this process; the PPB is required for orienting (before prophase) and guiding (in telophase) the mitotic apparatus. However, plants must possess additional mechanisms to control the division axis, as certain cell types or mutants do not form PPBs. Here, using live imaging of the gametophore of the moss *Physcomitrella patens*, we identified acentrosomal MTOCs, which we termed "gametosomes," appearing de novo and transiently in the prophase cytoplasm independent of PPB formation. We show that gametosomes are dispensable for spindle formation but required for metaphase spindle orientation. In some cells, gametosomes appeared reminiscent of the bipolar MT "polar cap" structure that forms transiently around the prophase nucleus in angiosperms. Specific disruption of the polar caps in tobacco cells misoriented the metaphase spindles and frequently altered the final division plane, indicating that they are functionally analogous to the gametosomes. These results suggest a broad use of transient MTOC structures as the spindle orientation machinery in plants, compensating for the evolutionary loss of centrosomes, to secure the initial orientation of the spindle in a spatial window that allows subsequent fine-tuning of the division plane axis by the guidance machinery.

asymmetric cell division | spindle orientation | MTOC | *Physcomitrella patens* | γ-tubulin

How do plants set their spindle division axis without centrosomes? In many angiosperm cell types, the cortical microtubules (MTs) are reorganized in G2 phase into a MT-based ring structure, the preprophase band (PPB), which encircles the nucleus at the cell cortex and represents a unique and key structure for oriented divisions in plants (1, 2). The PPB gradually degenerates during prophase. However, it defines the future division zone by recruiting a specific set of proteins to the cortex (3–8). During telophase, the phragmoplast, the postanaphase mitotic apparatus that recruits membrane and cell plate material for cytokinesis, centrifugally expands toward the cell cortex and strikingly precisely reaches the zone that the PPB formerly occupied. In addition to this "phragmoplast guidance" function, the PPB also sets initial spindle orientation. During degeneration of the PPB, nuclear envelope (NE)-associated MT structures, called polar caps, are formed on the opposite sides of the nucleus, perpendicular to the plane of the PPB (this structure is also called prospindle or prophase spindle) (9–12). *Arabidopsis* cell lines that do not assemble PPBs fail to establish these caps, indicating a critical role of the PPB in initial spindle orientation (9). However, whether initial spindle orientation by the PPB is critical for division plane determination is not clear, as the guidance mechanism could be strong enough to correct an initially misoriented mitotic appa-

ratus (13). Plants also must have developed a PPB-independent mechanism for division plane determination, as PPBs are not observed in certain plant cell types, such as gametophytic cells or endosperm cells that execute oriented divisions (14). For instance, without centrosomes or the PPB, the chloronemal apical cells of moss invariably orient the spindle along the cell's long axis and the division plane perpendicular to it (15, 16). Moreover, the recently reported *trm678* mutant that does not form obvious PPBs only causes some loss of precision in division plane orientation and develops remarkably normally (17). Overall, the mechanism of division axis determination is still not well understood in plants.

In this study, we aimed to uncover a fundamental mechanism of division plane determination in plants, and took the gametophore tissue of the moss *Physcomitrella patens* as model system (18). Multiple cell types in gametophores execute asymmetric cell division, and the tissue shows 3D growth to make the stem and leaf-like structures (19). We followed MT organization and cell division in the living gametophore. PPBs were not observed in every cell, but regardless of the presence or absence of PPBs, discrete cytoplasmic MT organizing centers (MTOC) were identified during prophase. The specific disruption of this structure during live imaging showed that the structure is a key determinant of spindle and division plane orientation. Analogous to this finding, when the polar caps were disrupted in tobacco BY-2 cells, spindle orientation was skewed and the cell plate was not accurately directed to the cortical division zone (CDZ) preestablished by the PPB. These

Significance

Cell division axis orientation is critical for differentiation and morphogenesis. In animal cells, centrosome-driven mitotic spindle orientation is key to orient cell divisions. However, in naturally acentrosomal plants, the mechanism underlying spindle orientation is poorly understood. Using two model systems, asymmetrically dividing cells in the moss *Physcomitrella patens* and tobacco tissue culture cells, we identified de novo assembled microtubule organizing centers during mitotic prophase as a common critical mechanism for spindle orientation. Disruption of these microtubule organizing centers caused misoriented spindles and cell plates. The "phragmoplast guidance" mechanism, which directs cell plate orientation, could not fully restore initial spindle orientation defects. Thus, this study identifies spindle orientation as a conserved factor in land plants to assist division plane orientation.

results suggest that acentrosomal MT assembly in prophase controls spindle orientation and that the spindle orientation is the first key step toward proper cell plate guidance in a wide range of plant cells.
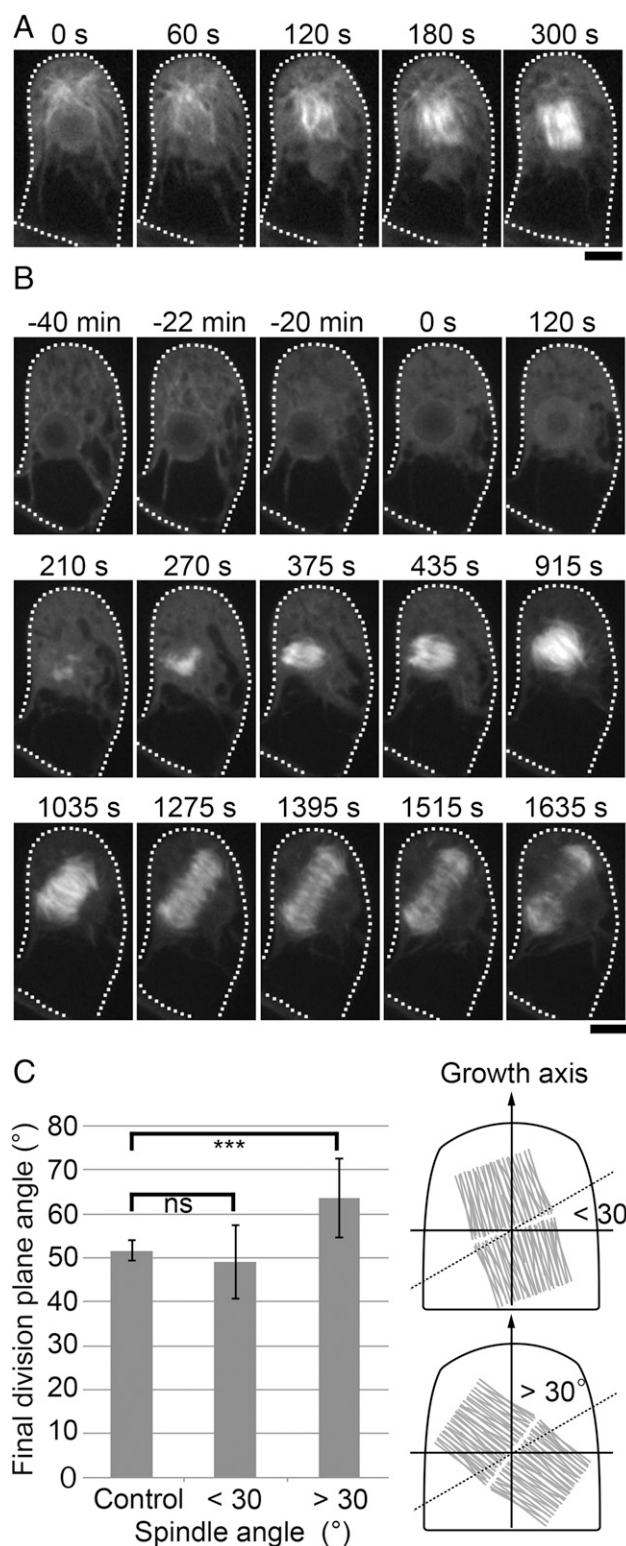
Results

The First Three Asymmetric Cell Divisions in the Gametophore Occur in a PPB-Independent Manner. *P. patens* has two distinct gametophyte bodies: the protonemata and the gametophores. Protonemata show filamentous tip growth (2D), whereas the gametophore, which differentiates from the protonemata, shows 3D growth to make the stem and leaf-like structures (19). We first aimed to study the first three asymmetric cell divisions in the gametophore, in which we observed that the division plane orientation is robustly determined, with small angle variations among independent gametophores (Fig. S1). We generated a transgenic moss line that expresses mCherry–α-tubulin and Citrine-MAP65d in the gametophore to monitor the determination process of the cell division plane in the gametophore initial cells. MAP65d is an MT-bundling protein weakly associated with the metaphase spindle midzone and strongly with the phragmoplast equator, enabling accurate measurement of the cell plate orientation relative to the cell growth axis (20). MAP65 also serves as a marker of the PPB and the cortical MT array in seed plants (21). The transgenic moss line grew with normal morphology, indicating that the transgenes did not significantly perturb MT dynamics or organization (Fig. S2A).

We performed time-lapse imaging at 2-min intervals (Fig. 1 and Movie S1). During the first three division cycles, cortical MT arrays were not apparent and PPB-like structures were not observed. However, 17 ± 4 min ($\pm$SD, $n = 23$) before the first division, a prominent MT cloud appeared in the cytoplasm at the apical side (−20 min in Fig. 1A). The cloud had a dense interior signal connected with MTs in various directions (*Inset* of Fig. 1A). The distance between the MT cloud and the nucleus gradually reduced, followed by NE breakdown (NEBD) and bipolar spindle formation (Fig. 1E). The spindle axis of the first divisions deviated by $17 \pm 8°$ ($\pm$SD, $n = 5$) from the apical–basal growth axis, and this orientation was maintained until anaphase onset. The phragmoplast formed in this orientation and rotated additionally $35 \pm 7°$ ($\pm$SD, $n = 5$) during its expansion to produce an oblique division plane (12–20 min in Fig. 1A). A single polar cytoplasmic MT cloud was also observed before the second and third division in the gametophore initial cells (Fig. 1 B and C and Movie S1).

To eliminate the possibility that the MT cloud assembly is an artifact of mCherry–α-tubulin expression, we immunostained endogenous MTs during the first gametophore division in wild-type moss cells (Fig. S2B). To identify prophase cells, we counterstained phosphorylated histone H3 at Ser10, which gets phosphorylated upon entry into mitosis (22). We observed the cytoplasmic MT cloud at prophase after immunostaining, indicating that they are formed in wild-type moss (Fig. S2B). This experiment also confirmed that PPBs do not form in the gametophore initial
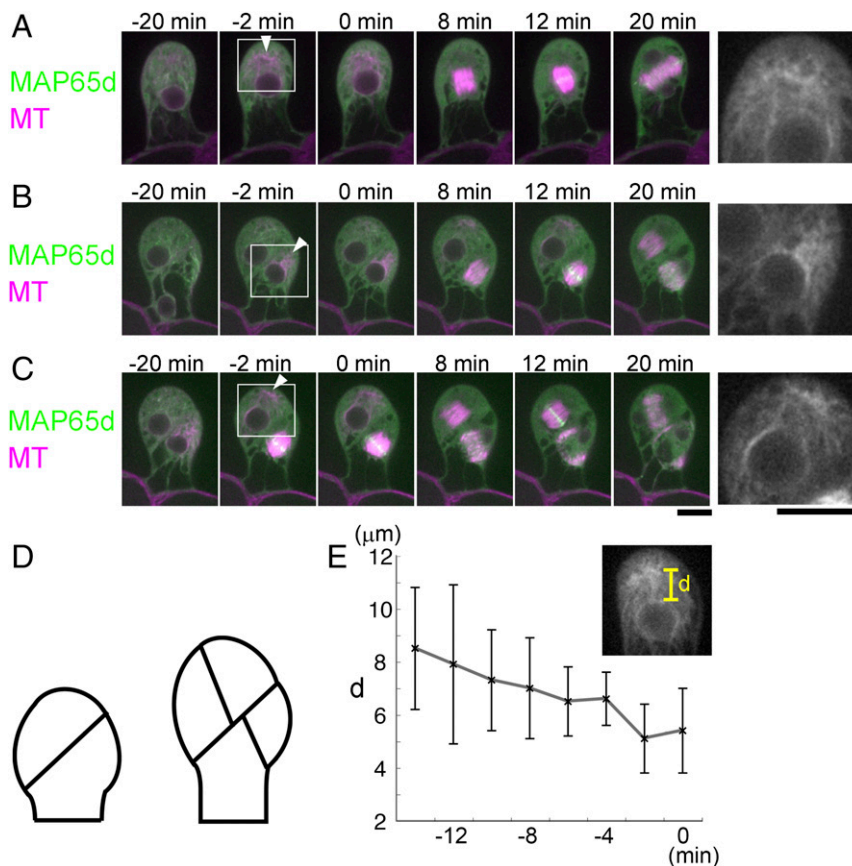
Fig. 1. A distinct MT organizing center appears during the asymmetric cell divisions of the gametophore initial. (*A–C*) Time-lapse imaging of Citrine-MAP65d (green) and mCherry–α-tubulin (magenta) during the first (*A*), second (*B*), and third (*C*) division in the gametophore initial. The gametophore in *B* is identical to the one shown in *C*. Images were recorded every 2 min. Time 0 corresponds to the timing of NEBD. Arrowheads indicate the MT cloud. Magnified views of the boxed regions are shown on the right. (Scale bars, 10 μm.) (*D*) Schematic representation of the initial division plane orientations in the gametophore. (*E*) Gradual decrease of the distance (d) between the MT cloud and the apical surface of the nucleus (±SD, $n = 5$). Time 0 corresponds to the timing of NEBD.

cell, in contrast to the first division of the zygote in angiosperm cells that clearly uses a PPB-dependent mechanism (23).

The Gametosome, an MTOC in the Prophase Cytoplasm Required for Proper Spindle Orientation. To analyze the behavior of the MT cloud during spindle assembly, we imaged mCherry–α-tubulin at 15-s intervals (Fig. 2*A* and Movie S2). MTs penetrated the nuclear space at NEBD and constituted spindle MTs, indicating that the cloud acts as a major MT generation and organization center (60–120 s in Fig. 2*A*). However, unlike centrosomes or other well-studied MTOCs, MTs were loosely focused in the clouds and their center could not be unambiguously assigned. Furthermore, the MT cloud merged into the spindle MTs and was no longer detectable as a discrete MTOC at metaphase (300 s). We named this transient MT organizing center in the gametophore cytoplasm the "gametosome."

We assessed the function of the gametosome by transient MT destabilization (Fig. 2*B* and Movies S3 and S4). In this experiment, we treated the gametophore with oryzalin, an MT-destabilizing chemical, as soon as we detected an immature MT cloud in the apical cytoplasm, before the first division (−22 min in Fig. 2*B*). As expected and in contrast to the DMSO control, where gametosome-based spindle assembly took place and metaphase spindles were fully observed in a single focal plane ($n = 6$), MTs disappeared rapidly following oryzalin treatment (−20 min in Fig. 2*B*). When NEBD took place, indicated by the inflow of soluble mCherry–α-tubulin into the nucleus, we washed out the oryzalin solution or DMSO by medium exchange (0–120 s in Fig. 2*B*). In the oryzalin washed-out cells, MTs reappeared at the region formerly occupied by the nucleus (210 s). Subsequently, the number of MTs gradually increased and eventually a bipolar spindle formed (375 s). During this spindle assembly process, we did not observe a reemergence of the gametosome, indicating that bipolar spindles can assemble independently of the gametosome. We interpret that chromatin-mediated MT nucleation and subsequent amplification led to spindle formation, which is typical for animal cells in the absence of centrosomes (24, 25). In the cell displayed in Fig. 2*B*, the spindle angle was oriented at 76° with respect to the tangential of the growth axis, as determined in Fig. S1*C*. Subsequently, the division plane was not properly set (56° with respect to the tangential of the growth axis). Biological repetitions of this experiment revealed the establishment of various spindle angles after washout of oryzalin. We classified the cells according to the angle of their spindle (within 30° tilted or over 30° tilted), and division plane orientation was measured in those cells (Fig. 2*C*). The average division plane orientation of the cells, originating from spindles which were tilted below 30°, was not significantly different from that of control cells [$49 \pm 8°$ ($\pm$SD, $n = 5$) vs. $52 \pm 2°$ ($n = 5$) for control cells]. In contrast, the average division plane orientation of the cells, which had their spindles tilted over 30°, was $64 \pm 9°$ ($\pm$SD, $n = 5$), which was significantly different from the control cells (Fig. 2*C*). These results indicate that gametosome-dependent spindle orientation in the gametophore initial division provides an important contribution to division plane orientation.

γ-Tubulin, but Not Augmin, TON1, or F-Actin, Is Required for Gametosome Formation. We next searched for factors responsible for gametosome formation. As possible contributors, we picked up three MT-associated proteins: γ-tubulin, augmin, and TON1. In the mitotic

Fig. 2. The gametosome plays a critical role in spindle orientation. (*A*) Time-lapse imaging of mCherry–α-tubulin during the first division of the game-tophore initial. Images were recorded every 15 s. Time 0 corresponds to the timing of NEBD. MTs emanated from the gametosome penetrate into the nucleus upon NEBD. Subsequent MT amplification and bipolarization leads to metaphase spindle formation (300 s). (*B*) Time-lapse imaging of mCherry–α-tubulin in a cell transiently treated with oryzalin. Before the first division in the gametophore initial, cells were treated with 20 μM oryzalin (−22 min), which destabilized the gametosome. Oryzalin was washed out upon NEBD (time 0), and images were recorded every 15 s. MTs were nucleated in a gametosome-independent manner and a bipolar spindle was formed (375 s). However, the orientation of the spindle was ectopic, as was also the angle of the expanding phragmoplast. Cells are outlined with dotted lines. (Scale bars, 10 μm.) (*C*) Measurement of final division plane angle in cells transiently treated with oryzalin. The cells were classified according to their spindle angles, which were within 30° ($n = 5$) or over 30° ($n = 5$), after oryzalin washout. The final division plane angles of classified cells were compared with control cells ($n = 5$) using t test. ***$P < 0.02$; ns, $P > 0.5$. Illustration of the spindle angle (within 30° or over 30°) on the right of graph. The dotted line shows 30°, and the gray structure indicates the spindle.
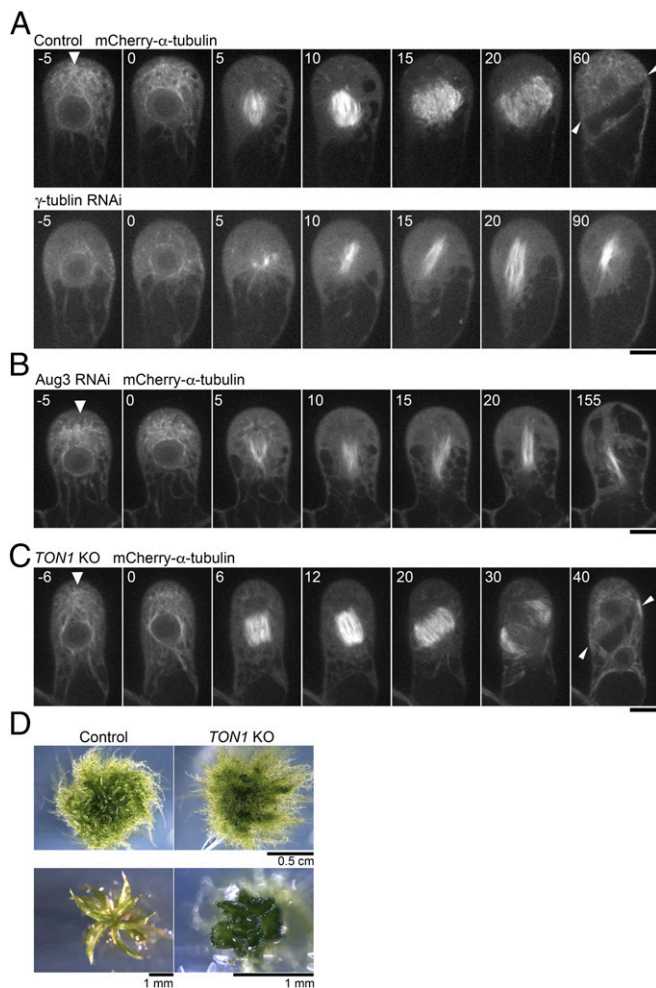
Fig. 3. γ-Tubulin is required for gametosome formation. (*A* and *B*) Time-lapse imaging of mCherry–α-tubulin during the first division of the gametophore initial in control, γ-tubulin RNAi, and Aug3 RNAi lines. Images were recorded every 5 min. Time 0 corresponds to the timing of NEBD. Arrowheads indicate gametosomes. (Scale bars, 10 μm.) (*C*) Time-lapse imaging of mCherry–α-tubulin during the first division in the gametophore initial of the *PpTON1*-deletion line. Images were recorded every 2 min. Time 0 corresponds to the timing of NEBD. The gametosome structure appears normally in prophase (arrowhead). (Scale bar, 10 μm.) (*D*) Abnormal gametophore morphology resulting from the *PpTON1* deletion, consistent with previously reported data (30). Arrowheads in the final frames of *A* and *C* show the final division plane orientation.

spindle, phragmoplast, and cortical MTs in seed plants, MT-dependent MT nucleation (also called branching nucleation) represents a predominant mode of MT nucleation. In this process, the protein complex augmin binds to existing MTs and recruits a potent MT nucleator, γ-tubulin (16, 26). This mechanism ensures efficient MT amplification. TON1 forms a complex with PP2A, regulates branching MT nucleation during interphase, and is required for PPB formation and oriented cell division (27–30). Our attempts to localize these proteins in the gametophore initial cell by immunostaining or Citrine tagging at the endogenous locus have been unsuccessful; signals were not detected anywhere above background autofluorescence. We therefore depleted those genes by RNAi (γ-tubulin and the Aug3 subunit of augmin) or gene disruption (TON1), and observed the MTs in living cells. We confirmed the appearance of the expected phenotype for these newly selected transgenic lines: defects in mitotic spindle assembly (γ-tubulin or Aug3 depletion) or gametophore development (TON1 deletion) (Fig. 3 and Movie S5). We observed lack of gametosome formation

only upon induced depletion of γ-tubulin (Fig. 3 *A–C*). Therefore, the gametosome is likely formed through a nonbranching-type of MT nucleation. Furthermore, the orientation of the spindle ($14° \pm 8$, $\pm$SD, $n = 5$) and the division plane ($52° \pm 2$, $n = 5$) in the absence of TON1 did not deviate significantly from the control situation ($16° \pm 5$, $\pm$SD; t test $P > 0.6$ and $51° \pm 4$; t test $P > 0.6$, respectively), emphasizing that spindle and division plane orientation of the first gametophore division in moss occurs via a PPB-independent mechanism.

The actin cytoskeleton also affects the orientation of the cell division axis in many cell types (31, 32). Specifically, actin microfilaments show a characteristic "twin peak" pattern at the cortex after the PPB disappears, with a minimum density at the zone where the PPB was previously located (i.e., the CDZ where the cell plate is guided to during cytokinesis). Treatment with actin polymerization inhibitors has been reported to cause cell plate misorientation, indicating that actin microfilaments are also critical factors for division plane determination (33–35). To investigate the involvement of actin microfilaments in division plane determination in the gametophore initial cell, we first determined the distribution of the actin microfilaments by imaging the Lifeact-GFP marker, which specifically stains filamentous actin (36). The appearance of a cortical zone with reduced actin microfilament density, analogous to the twin peaks pattern reported for BY-2 cells (35), was not detected throughout mitosis and no obvious accumulation of actin at the presumed position of the gametosome could be detected (Fig. 4*A*). We nevertheless observed strong GFP signals at the region corresponding to the
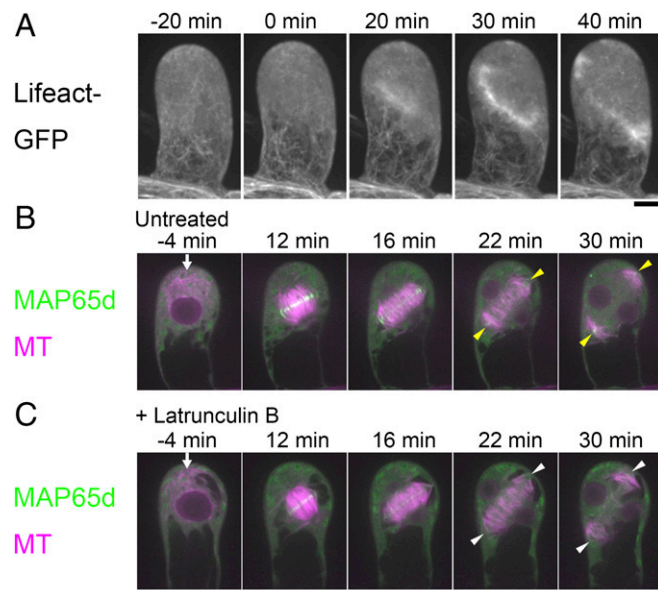
Fig. 4. Actin inhibition has little impact on division plane determination of the gametophore initial division. (*A*) Localization of actin filaments during the first gametophore division visualized by the Lifeact-GFP marker. No twin peaks pattern or accumulation at the presumed gametosome location could be observed. However, strong accumulation was seen at the phragmoplast midzone. Images were acquired every 5 min with 31 *z*-sections (separated by 1 μm) and displayed using maximum projection. Time 0 corresponds to the timing of NEBD. (*B* and *C*) Time-lapse imaging of mCherry–α-tubulin (magenta) and Citrine-MAP65d (green) during the first division in the gametophore initial with (*B*) or without (*C*) 25 μM of the actin inhibitor Latrunculin B. Images were recorded every 2 min. Time 0 corresponds to the timing of NEBD. Arrows indicate gametosomes. Yellow arrowheads indicate MT interdigitation at the leading edge of the phragmoplast, which have prominent Citrine-MAP65d signals. White arrowheads indicate abnormal MT interdigitations at the leading edge of the phragmoplast, which lack prominent Citrine-MAP65d signals. (Scale bars, 10 μm.)
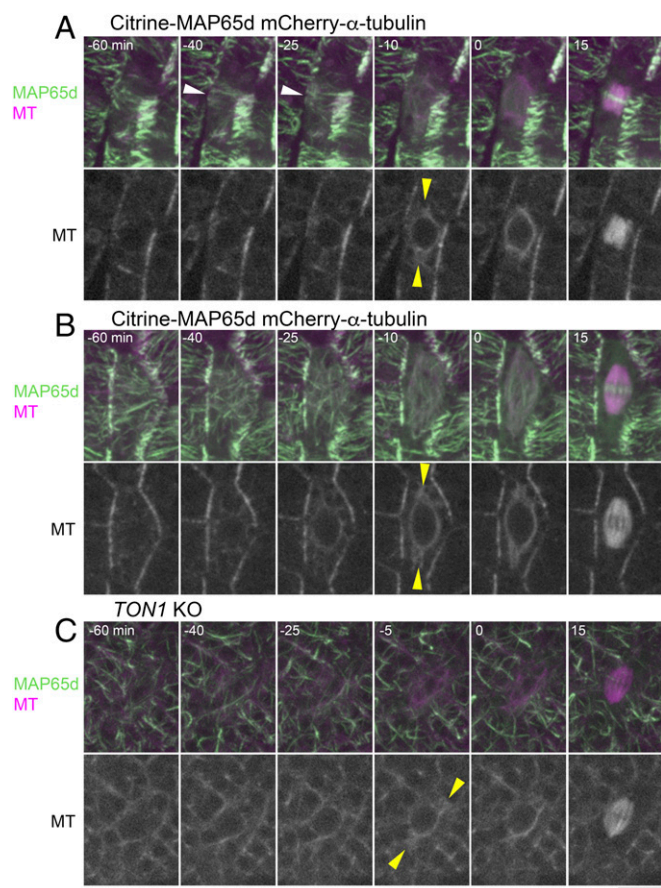
Fig. 5. Gametosome formation in leaf-like gametophore cells occurs independently of PPB formation. (*A* and *B*) Time-lapse imaging of Citrine-MAP65d (green) and mCherry–α-tubulin (magenta) in gametophore cells with (*A*) or without (*B*) PPB formation. Images were acquired every 5 min with 16 *z*-sections (separated by 1 μm) and displayed after maximum projection (*Top*, merged) or as single median slices (*Bottom*, grayscale). Time 0 corresponds to the timing of NEBD. PPBs (white) and gametosomes (yellow) are marked with arrowheads. (*C*) Time-lapse imaging of Citrine-MAP65d (green) and mCherry–α-tubulin (magenta) in gametophore cells of the *PpTON1*-deletion line. Images were acquired every 5 min with 21 *z*-sections (separated by 1 μm) and displayed after maximum projection (*Top*, merged) or as single median slices (*Bottom*, grayscale). Time 0 corresponds to the timing of NEBD. Gametosomes form in gametophore cells in this background and are marked with yellow arrowheads. (Scale bar, 10 μm.)

phragmoplast midzone (20–40 min). We next performed time-lapse imaging of mCherry–α-tubulin and Citrine-MAP65d after treatment with Latrunculin B, an actin microfilament destabilizer (Fig. 4 *B* and *C* and Movie S6). We identified mild defects in MT plus-end interdigitation at the leading edge of the phragmoplast during expansion (t = 22 min and 30 min) (arrowheads in Fig. 4 *B* and *C*). However, the gametosome appeared as normal (arrows at −4 min in Fig. 4 *B* and *C*), and the metaphase spindles were properly oriented (spindle angle of control cells 20° ± 10, ±SD; Lat B treated 17° ± 7; *t* test $P > 0.5$; $n = 5$ each), which led to the formation of phragmoplasts and division planes with proper orientation (angle α, defined in Fig. S1*C*, was 45° ± 9 in the control and 47° ± 13 in Lat B-treated cells; $n = 5$ each, *t* test $P > 0.8$). Gametosome appearance was also observed in the presence of another actin-destabilizing drug, Cytochalasin B (Fig. S3 *A* and *B*). We concluded that actin filaments are involved in ensuring the structural integrity of the phragmoplast, but play little role in gametosome formation, spindle orientation, or division plane determination in the initial gametophore divisions.

P. patens myosin VIII is an MT-associated myosin and is localized at the CDZ in the branch-forming cell of protonemata, where it guides phragmoplast MTs during expansion, and thereby controls division plane orientation (37). To investigate a possible contribution of myosin VIII to gametosome formation, we immunostained MTs in the *myo8*-null line (quintuple *myo8ABCDE* deletion line). We observed the gametosome in prophase cells, indicating that, in agreement with the results using actin destabilizing drugs, Myo8 is dispensable for gametosome formation at this stage (Fig. S3*C*).

The PPB and Gametosome Control Cell Division Orientation in Leaf-Like Gametophore Cells. Previous studies, using immunofluorescence microscopy of MTs, identified PPBs in the leaf-like gametophore cells of the *P. patens* gametophore (30, 38). This suggests that the PPB controls the cell division axis in this tissue; whether polar caps or equivalent structures are assembled was not clarified. To address how the gametosome-based mechanism of the first three divisions switches to a PPB-based mechanism during gametophore development, we performed live-cell time-lapse imaging of leaf-like gametophore cells at 5-min intervals, using the mCherry–α-tubulin and Citrine-MAP65d marker line (Fig. 5, Figs. S4 and S5, and Movie S7). We observed PPBs before NEBD in about only a half of the cells (30 of 56). Twenty-five of these cells showed bands of MTs somewhat resembling PPBs in seed plants (white arrowheads in Fig. 5*A*, Fig. S4 *B–D* and *H*, and Movie S7), whereas five other cells exhibited only broad bands, which were difficult to discriminate from the interphase cortical MT organization (Fig. S4 *A* and *E–G*). Overall, PPBs were never as dense and clearly defined as in angiosperm cells. The PPBs disappeared at −13 ± 6 min (±SD, $n = 27$) before NEBD. Notably, we observed one to three discrete MTOCs in the cytoplasm closer to NEBD (at 15–5 min before) in 21 of these cells. The structures were similar to those observed in the gametophore initials, and served as the poles of the spindles upon NEBD (Fig. 5*A*, yellow arrowheads). Thus, they could also be referred to as gametosomes. However, the number and position of these gametosomes were imprecisely set; for example, in six cells we observed >two gametosomes, leading to multipolar spindle formation immediately following NEBD (Fig. S4 *G* and *H*). The occurrence of initially multipolar spindles being formed suggests that the moss PPB cannot accurately control spindle bipolarity. The remaining nine cells assembled MTs around the nucleus in prophase, in which we detected more intense MT signals at two sites than in other areas (Fig. S4*D*). They subsequently became the two poles of the spindle, reminiscent of the polar caps of angiosperms.

In contrast, we could not identify PPBs in the other 26 cells (Fig. 5*B*, Fig. S5, and Movie S7). This was either because these cells did not form PPBs or our imaging conditions failed to visualize the faint and transient structure. Regardless, we observed gametosomes in 21 of 26 of these cells, and the initial spindle orientation was consistent with their position (yellow arrowheads in Fig. 5*B* and Fig. S5 *A*, *C*, and *D*). These results suggest that, similar to the situation in the first gametophore divisions, the PPB is not essential for the formation of gametosomes in the leaf-like gametophore cells. In the remaining five cells, we failed to identify clearly defined gametosomes (Fig. S5 *B* and *E*). However, these cells assembled MTs around the nucleus in prophase.

To clarify the relationship between gametosomes and the PPB, we performed live-cell imaging in leaf-like gametophore cells in the *TON1* knockout mutant (Fig. 5*C*). We could not detect PPBs in this background, but two gametosomes were visible before NEBD and the initial spindle orientation was consistent with their position ($n = 11$) (Fig. 5*C*).

These results indicate that in moss gametophore cells, gametosomes can form in the absence of a PPB and steer the initial spindle orientation. Moreover, even in cells that form PPBs, the position and the number of gametosomes have a more pronounced influence on initial spindle formation than the PPB does.

The Polar Cap of Tobacco Cells Is a Critical Determinant of Spindle and Cell Division Axes. The gametosome has a noticeable similarity to the MT-based polar cap structure in flowering plants, which is formed at prophase in a PPB-dependent manner at opposite locations at the NE (9, 10, 39, 40). Polar caps supply spindle MTs during spindle assembly, but are eventually integrated into the main body of the spindle, similar to the gametosomes. Furthermore, cultured *Arabidopsis* cells lacking polar caps as well as PPBs display spindle misorientation and enhanced phragmoplast mobility (9). However, it is unknown whether specific disruption of the polar caps, without disrupting the PPB or inhibiting the recruitment of cell plate guidance factors, results in spindle or phragmoplast misorientation, as was observed for the gametosome.

To assess a role of the polar caps in division plane determination via controlling the initial spindle orientation without abolishing the cell plate guidance mechanism, we performed a MT depolymerization-regrowth assay in tobacco BY-2 cells expressing an MT marker. As expected, in control cells ($n = 7$) the majority ($n = 5$) of cells formed their spindle and phragmoplast perpendicular to the PPB, and the cell plate expanded to the location of the former PPB (Fig. 6A). In drug washout cells ($n = 9$), MTs reappeared at the region formerly occupied by the nucleus and eventually bipolar spindles were formed (Fig. 6 B and C, 12–26 min) (propyzamide was used instead of oryzalin to depolymerize MTs). However, eight of nine spindles were improperly oriented (26 min in Fig. 6 B and C). These results were identical to what was observed in the gametophore initials, supporting the hypothesis that polar caps and gametosomes are analogous structures required for spindle orientation.

Bipolar spindles formed after drug washout were converted to phragmoplasts. MT depolymerization has been previously shown not to affect the localization of CDZ markers, which are required for phragmoplast guidance (3, 5). We confirmed that the signal intensity of GFP-TAN1, a CDZ marker, did not significantly change during the length of our drug treatment (Fig. 6 D and E).

Of eight cells that were monitored following propyzamide treatment, the phragmoplasts of four cells rotated and eventually reached the correct insertion sites previously marked by the PPB, and thus rescued the aberrant initial spindle orientation (Fig. 6C). However, the four other cells could not rescue the initially defective spindle orientation despite rotation of the phragmoplast, and finished cytokinesis with ectopically oriented cell plates (Fig. 6B). Thus, chromosomal-based spindle formation alone is not sufficient for proper division plane orientation, as the correctional capacity of the phragmoplast guidance mechanism has limitations.

Discussion

This study identified the gametosome as the determinant of spindle orientation contributing to division plane determination in moss gametophore cells. Our live-cell imaging data of the first gametophore division reveals that the formation and localization of the gametosome is key to set the initial spindle axis as the mitotic spindle emerges along the gametosome–nucleus axis and that the initial spindle orientation assists in division plane orientation. We further observed rotation of the phragmoplast with respect to the initial spindle orientation. Gametosome-based spindle orientation therefore likely cooperates with additional mechanisms, fine-tuning division plane orientation during the first gametophore divisions, which we found are TON1- and PPB-independent. Our results showing normal division plane orientation in a *ton1* mutant background disagree with a previous report (30). The reason for this discrepancy is unclear and might be explained by different gametophore induction conditions or by the different knockout strategy used. Gametophore cell patterning is affected in both *ton1* mutants, given the clearly aberrant macroscopical phenotype of the leaf-like gametophore. Our data point to these defects occurring after the initial rounds of gametophore divisions.
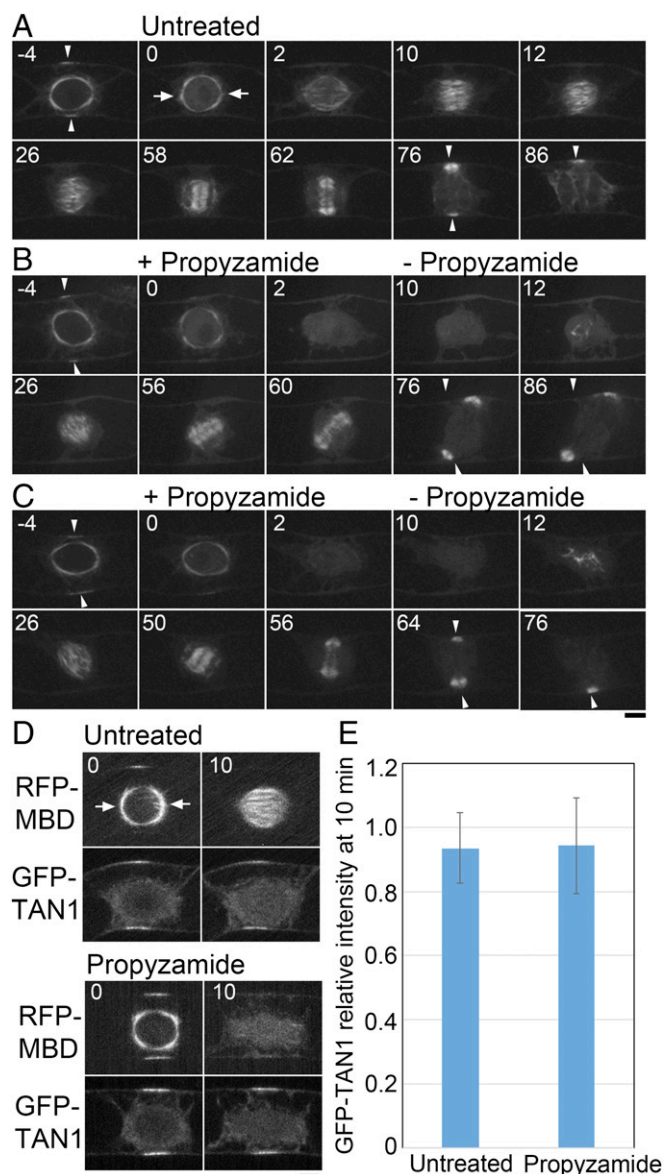
Fig. 6. Polar cap-dependent spindle orientation contributes to division plane control in tobacco BY-2 cells. (*A–C*) Time-lapse imaging of YFP-β-tubulin in a control untreated cell (*A*) and upon transient treatment with propyzamide (*B* and *C*). Before NEBD (time 0), cells were treated with 10 μM propyzamide that destabilized the polar caps. Propyzamide was washed out after cells were allowed to progress past NEBD for 10 min, and images were recorded every 30 s. MTs were nucleated in a polar cap-independent manner and a bipolar spindle formed (26 min). However, orientation of the spindle was random. In the cell presented in *C*, the division plane was eventually corrected by phragmoplast guidance toward the region where PPB was formerly present (50–64 min), whereas in *B* the guidance mechanism was not sufficient to correct the plane (76 min). Arrowheads indicate the PPB and the corresponding region marked by PPB before NEBD. Arrows indicate polar caps. (Scale bar, 10 μm.) (*D*) Representative images of BY-2 cells expressing RFP-MBD and the CDZ marker GFP-TAN1 in a control untreated cell and upon transient treatment with propyzamide. Time is indicated in minutes. (Scale bar, 10 μm.) (*E*) Quantification of GFP-TAN1 intensity at the CDZ of untreated and treated BY-2 cells. The ratio of the fluorescence intensity between time point 0 min and time point 10 min is shown with SD ($n = 10$). Arrows indicate the polar caps.

It remains unclear how cells determine where the gametosome is assembled and why there is only one in the first divisions, whereas two or even multiple ones appear when the leaf-like gametophore cells divide. Nevertheless, our localization and

genetic data demonstrate that in the first gametophore divisions, a single gametosome is localized in the apical cytoplasm, independent of a PPB. The PPB might help the determination of gametophore localization in late gametophore cells, like it facilitates polar cap formation in angiosperms (9–12). However, the localization of the gametosome is also PPB-independent in some wild-type leaf-like gametophore cells where gametosomes formed in the central area of the wide-open cytoplasmic space. Moreover, gametosomes were clearly visible in the leaf-like gametophore cells of the *ton1* knockout line, indicating that their formation does not require a PPB.

Mechanistically, gametosome formation requires γ-tubulin but not augmin. Thus, activation of nonbranched-type MT nucleation in the prophase cytoplasm and motor-dependent MT clustering (41) might be sufficient to self-organize a single gametosome structure in the cytoplasmic compartment. Identification of the genes required for the localization of gametosome would be an important next step toward molecular understanding of the mechanism underlying spindle orientation in the gametophore and, more broadly, the execution of asymmetric divisions.

In the first gametophore division, the deviation in the angle of the spindle, generated in the absence of the gametosome was correlated with cell plate misorientation. Similarly, in BY-2 cells, spindles forced to form without polar caps, and thereby lacking any orientation information from the PPB, were also oriented randomly, and this often led to ectopic cell plate insertion. Thus, we suggest that polar caps in tobacco cells have an analogous function to gametosomes. Our results that the polar caps play a decisive role in spindle orientation are in agreement with previous reports on the *Arabidopsis* kinesin-14 mutant, *Atk5-1*, which shows defects in spindle length, pole width, and integrity at prometaphase, but is not defective in pole focusing before NEBD and also does not cause obvious division plane orientation defects (42, 43).

Notably, in liverworts, two aster-like structures, called polar organizers, emerge on opposite sides of the nucleus before the PPB appearance (i.e., independent of the PPB function) (44–47). Although not experimentally addressed, it is tempting to speculate that polar organizers also function as the main determinants of spindle orientation in liverworts. The identification of the gametosome in moss, functioning in initial spindle orientation and thereby contributing to division plane orientation both with and without PPB formation, supports the idea of a stepwise rather than a sudden transition between ancient (centrosomal) and modern (PPB-dependent) mechanisms of cell division in the green lineage (48).

In conclusion, our observations suggest that cytoplasmic MTOC-based mechanisms for spindle orientation are conserved among land plants. Loss of centrosomes during plant evolution may have been compensated by the development or retention of an acentrosomal MTOC structure with an analogous function to the centrosome.

Materials and Methods

Transgenic Lines. The primers for plasmid construction are shown in Table S1. To generate Citrine-SYP1a and Citrine-MAP65d lines, we amplified genomic DNA sequences upstream and downstream of their start codons with specific primers and cloned them into the pKK138 vector (20). To generate *TON1* knockout lines, the amplified upstream/downstream sequences were cloned into pTN186. mCherry–α-tubulin and Lifeact-GFP were cloned into a vector that contained the *EF1α* promoter. The plasmids were integrated at a nonnative locus. The standard polyethylene glycol-mediated procedure was used for the transformation of the wild-type strain of *P. patens* subsp. *patens* (16, 20, 49). Inducible RNAi lines for γ-tubulin and augmin were selected by the method following ref. 16. In brief, RNAi constructs (used in ref. 16) were cloned into the pGG624 vector (50), and the plasmid was transformed into Citrine-MAP65d/mCherry–α-tubulin line after PmeI digestion. Transgenic lines were selected based on hygromycin resistance, and the RNAi lines were selected after long-term imaging (3-min intervals, 10 h) of protonemata and assessment of the mitotic phenotypes (prolonged prometaphase and formation of an abnormally long spindle). The YFP–β-tubulin expression line of tobacco BY-2 cells was made with a binary plasmid pBI1214-YFPTUB (51). The

GFP-TAN1/RFP-MBD cell line was made by sequential BY-2 transformation (p35S::GFP-TAN1 was transformed into a previously established p35S::RFP-MBD-expressing BY-2 line). The p35S::RFP-MBD and the p35S::GFP-TAN1 constructs were described elsewhere (3, 52, 53).

Microscopy. Protonemal cells were cultured at 24–25 °C on glass-bottom plates covered with the BCD agar medium for 5 d (49). The gametophore initial was observed in 5-d-old protonemal cells that were cultured for 22–24 h in the presence of 1 μM benzylaminopurine (BAP) synthetic cytokinin. For the MT depolymerization-regrowth experiment in the gametophore initial, oryzalin was dissolved in DMSO at a concentration of 1 mM and added at a 1:1,000 dilution to the BCD medium. Latrunculin B was dissolved in DMSO at a concentration of 25 mM and added at a 1:1,000 dilution to the BCD medium. Effectiveness of latrunculin B was confirmed with the treatment of the Lifeact-GFP line. Cytochalasin B was diluted in DMSO at a concentration of 20 mM and added at a 1: 100 dilution to the BCD medium. The diluted solution was added to the culture plate 10–20 min before the timing of NEBD. When we observed NEBD, we washed out oryzalin by replacing the BCD medium four times. For the MT depolymerization-regrowth experiment in the BY-2 cell lines, 10 μM propyzamide was applied to the cells attached onto a poly-lysine–coated, grass-bottom dish (54) at NEBD. Cells were allowed to progress past NEBD for 10 min before washout started. To wash out propyzamide, the medium was replaced with a drug-free medium six times: 0.8 mL of the medium was added by a pipetman while it was continuously aspirated with a pump. To observe the leaf-like gametophore cells, protonemal cells were directly put on the glass-bottom plates, and then covered with the BCD agarose medium (the low melting point agarose was used). The plates were inverted and cultured for 3–4 d. We used a fluorescent marker, Citrine-MAP65d, to identify the gametophore, which is naturally developed from the protonemal tissue (BAP was untreated). MAP65d is expressed in gametophores, but not in protonemata (20). In the time-lapse imaging at 5-min intervals, white light was illuminated for 3 min between Citrine/mCherry image acquisitions. A Nikon TE2000 microscope equipped with a CSU-X spinning-disk confocal unit (Yokogawa) and an electron-multiplying charge-coupled device camera (ImagEM; Hamamatsu) was used for live imaging of the gametophore initial (40×, 1.30-NA lens). The microscope was controlled using the Micromanager software. For the observation of gametophore cells, a Nikon Ti-E microscope equipped with CSU-X and ImagEM was used for live imaging (60×, 1.2-NA lens). The microscope was controlled using the Volocity software package (Perkin-Elmer). The spindle and final division angles were measured after 3D projection using ImageJ (axis of rotation = y axis). For image acquisition of tobacco suspension culture cells in a single color, an Olympus IX81 microscope equipped with a CSU21 spinning-disk confocal unit (Yokogawa) and a SCMOS camera (Orca-Flash 4.0; Hamamatsu) was used with a 60× objective (NA 1.2). For dual-color acquisition, a Nikon A1 confocal microscope with GaASP photo-multipliers was used with a 60× objective (NA 1.2). Immunostaining of α-tubulin and phosphorylate Ser10 of histone H3 was performed as described previously (16, 55) with slight modification. In brief, cytokinin-induced gametophores or 4-d-old cultured gametophores were fixed with 8% paraformaldehyde, 100 mM Pipes-NaOH, pH 6.8, 2.5 mM EGTA, 1 mM MgCl$_2$, 1% DMSO, and 0.1% Nonidet P-40 for 1 h. Cell walls were digested with 2% (wt/vol) driselase at 37 °C for 1 h. The cells were incubated with 1:300 dilution of anti–α-tubulin antibody (YOL1/34; Merck Millopore) and 1:300 dilution of antiphospho-histone H3 (Ser10) antibody (Rabbit polyclonal antibody; Merck Millopore) in PBS overnight at 4 °C. GFP-TAN1 fluorescence of the tobacco cell line was analyzed with ImageJ. After subtraction of background fluorescence (average intensity of a region of interest outside the cell area), the sum of grayscale pixel values of the CDZ was quantified, and relative intensities at 10 min to 0 min after NEBD were determined.

1. Mineyuki Y (1999) The preprophase band of microtubules: Its function as a cytokinetic apparatus in higher plants. *Int Rev Cytol* 187:1–49.

2. Pickett-Heaps JD, Northcote DH (1966) Organization of microtubules and endoplasmic reticulum during mitosis and cytokinesis in wheat meristems. *J Cell Sci* 1:109–120.

3. Lipka E, et al. (2014) The phragmoplast-orienting kinesin-12 class proteins translate the positional information of the preprophase band to establish the cortical division zone in *Arabidopsis thaliana*. *Plant Cell* 26:2617–2632.

4. Vanstraelen M, et al. (2006) Cell cycle-dependent targeting of a kinesin at the plasma membrane demarcates the division site in plant cells. *Curr Biol* 16:308–314.

5. Walker KL, Müller S, Moss D, Ehrhardt DW, Smith LG (2007) *Arabidopsis* TANGLED identifies the division plane throughout mitosis and cytokinesis. *Curr Biol* 17:1827–1836.

6. Xu XM, et al. (2008) RanGAP1 is a continuous marker of the *Arabidopsis* cell division plane. *Proc Natl Acad Sci USA* 105:18637–18642.

7. Buschmann H, et al. (2015) *Arabidopsis* KCBP interacts with AIR9 but stays in the cortical division zone throughout mitosis via its MyTH4-FERM domain. *J Cell Sci* 128:2033–2046.

8. Stöckle D, et al. (2016) Putative RopGAPs impact division plane selection and interact with kinesin-12 POK1. *Nat Plants* 2:16120.

9. Chan J, Calder G, Fox S, Lloyd C (2005) Localization of the microtubule end binding protein EB1 reveals alternative pathways of spindle development in *Arabidopsis* suspension cells. *Plant Cell* 17:1737–1748.

10. Ambrose JC, Cyr R (2008) Mitotic spindle organization by the preprophase band. *Mol Plant* 1:950–960.

11. Liu B, Marc J, Joshi HC, Palevitz BA (1993) A gamma-tubulin-related protein associated with the microtubule arrays of higher plants in a cell cycle-dependent manner. *J Cell Sci* 104:1217–1228.

12. Zhang D, Wadsworth P, Hepler PK (1990) Microtubule dynamics in living dividing plant cells: Confocal imaging of microinjected fluorescent brain tubulin. *Proc Natl Acad Sci USA* 87:8820–8824.

13. Palevitz BA, Hepler PK (1974) Control of plane of division during stomatal differentiation in Allium. 1. Spindle reorientation. *Chromosoma* 46:297–326.

14. Otegui M, Staehelin LA (2000) Cytokinesis in flowering plants: More than one way to divide a cell. *Curr Opin Plant Biol* 3:493–502.

15. Doonan JH, Cove DJ, Lloyd CW (1985) Immunofluorescence microscopy of microtubules in intact cell lineages of the moss, *Physcomitrella patens*. I. Normal and CIPC-treated tip cells. *J Cell Sci* 75:131–147.

16. Nakaoka Y, et al. (2012) An inducible RNA interference system in *Physcomitrella patens* reveals a dominant role of augmin in phragmoplast microtubule generation. *Plant Cell* 24:1478–1493.

17. Schaefer E, et al. (2017) The preprophase band of microtubules controls the robustness of division orientation in plants. *Science* 356:186–189.

18. Rensing SA, et al. (2008) The *Physcomitrella* genome reveals evolutionary insights into the conquest of land by plants. *Science* 319:64–69.

19. Cove DJ, Knight CD (1993) The moss *Physcomitrella patens*, a model system with potential for the study of plant reproduction. *Plant Cell* 5:1483–1488.

20. Kosetsu K, de Keijzer J, Janson ME, Goshima G (2013) MICROTUBULE-ASSOCIATED PROTEIN65 is essential for maintenance of phragmoplast bipolarity and formation of the cell plate in *Physcomitrella patens*. *Plant Cell* 25:4479–4492.

21. Lucas JR, Shaw SL (2012) MAP65-1 and MAP65-2 promote cell proliferation and axial growth in *Arabidopsis* roots. *Plant J* 71:454–463.

22. Houben A, et al. (1999) Short communication: The cell cycle dependent phosphorylation of histone H3 is correlated with the condensation of plant mitotic chromosomes. *Plant J* 18:675–679.

23. Kimata Y, et al. (2016) Cytoskeleton dynamics control the first asymmetric cell division in *Arabidopsis* zygote. *Proc Natl Acad Sci USA* 113:14157–14162.

24. Heald R, et al. (1996) Self-organization of microtubules into bipolar spindles around artificial chromosomes in *Xenopus* egg extracts. *Nature* 382:420–425.

25. Goshima G, Mayer M, Zhang N, Stuurman N, Vale RD (2008) Augmin: A protein complex required for centrosome-independent microtubule generation within the spindle. *J Cell Biol* 181:421–429.

26. Liu T, et al. (2014) Augmin triggers microtubule-dependent microtubule nucleation in interphase plant cells. *Curr Biol* 24:2708–2713.

27. Azimzadeh J, et al. (2008) *Arabidopsis* TONNEAU1 proteins are essential for preprophase band formation and interact with centrin. *Plant Cell* 20:2146–2159.

28. Kirik A, Ehrhardt DW, Kirik V (2012) TONNEAU2/FASS regulates the geometry of microtubule nucleation and cortical array organization in interphase *Arabidopsis* cells. *Plant Cell* 24:1158–1170.

29. Spinner L, et al. (2013) A protein phosphatase 2A complex spatially controls plant cell division. *Nat Commun* 4:1863.

30. Spinner L, et al. (2010) The function of TONNEAU1 in moss reveals ancient mechanisms of division plane specification and cell elongation in land plants. *Development* 137:2733–2742.

31. Panteris E (2008) Cortical actin filaments at the division site of mitotic plant cells: A reconsideration of the 'actin-depleted zone'. *New Phytol* 179:334–341.

32. Kunda P, Baum B (2009) The actin cytoskeleton in spindle assembly and positioning. *Trends Cell Biol* 19:174–179.

33. Cleary AL, Gunning BES, Wasteneys GO, Hepler PK (1992) Microtubule and F-actin dynamics at the division site in living tradescantia stamen hair cells. *J Cell Sci* 103:977–988.

34. Hoshino H, Yoneda A, Kumagai F, Hasezawa S (2003) Roles of actin-depleted zone and preprophase band in determining the division site of higher-plant cells, a tobacco BY-2 cell line expressing GFP-tubulin. *Protoplasma* 222:157–165.

35. Sano T, Higaki T, Oda Y, Hayashi T, Hasezawa S (2005) Appearance of actin microfilament 'twin peaks' in mitosis and their function in cell plate formation, as visualized in tobacco BY-2 cells expressing GFP-fimbrin. *Plant J* 44:595–605.

36. Vidali L, Rounds CM, Hepler PK, Bezanilla M (2009) Lifeact-mEGFP reveals a dynamic apical F-actin network in tip growing plant cells. *PLoS One* 4:e5744.

37. Wu SZ, Bezanilla M (2014) Myosin VIII associates with microtubule ends and together with actin plays a role in guiding plant cell division. *Elife* 3:e03498.

38. Doonan JH, Cove DJ, Corke FMK, Lloyd CW (1987) Pre-prophase band of microtubules, absent from tip-growing moss filaments, arises in leafy shoots during transition to intercalary growth. *Cell Motil Cytoskeleton* 7:138–153.

39. Liu B, et al. (1994) gamma-Tubulin in *Arabidopsis*: Gene sequence, immunoblot, and immunofluorescence studies. *Plant Cell* 6:303–314.

40. Lloyd C, Chan J (2006) Not so divided: The common basis of plant and animal cell division. *Nat Rev Mol Cell Biol* 7:147–152.

41. Surrey T, Nedelec F, Leibler S, Karsenti E (2001) Physical properties determining self-organization of motors and microtubules. *Science* 292:1167–1171.

42. Ambrose JC, Cyr R (2007) The kinesin ATK5 functions in early spindle assembly in *Arabidopsis*. *Plant Cell* 19:226–236.

43. Ambrose JC, Li W, Marcus A, Ma H, Cyr R (2005) A minus-end-directed kinesin with plus-end tracking protein activity is involved in spindle morphogenesis. *Mol Biol Cell* 16:1584–1592.

44. Brown RC, Lemmon BE (1990) Polar organizers mark division axis prior to preprophase band formation in mitosis of the hepatic *Reboulia hemisphaerica* (Bryophyta). *Protoplasma* 156:74–81.

45. Brown RC, Lemmon BE (2011) Dividing without centrioles: Innovative plant microtubule organizing centres organize mitotic spindles in bryophytes, the earliest extant lineages of land plants. *AoB Plants* 2011:plr028.

46. Buschmann H, Holtmannspötter M, Borchers A, O'Donoghue MT, Zachgo S (2016) Microtubule dynamics of the centrosome-like polar organizers from the basal land plant *Marchantia polymorpha*. *New Phytol* 209:999–1013.

47. Brown RC, Lemmon BE, Horio T (2004) Gamma-tubulin localization changes from discrete polar organizers to anastral spindles and phragmoplasts in mitosis of *Marchantia polymorpha* L. *Protoplasma* 224:187–193.

48. Buschmann H, Zachgo S (2016) The evolution of cell division: From streptophyte algae to land plants. *Trends Plant Sci* 21:872–883.

49. Ashton NW, Cove DJ (1977) Isolation and preliminary characterization of auxotrophic and analog resistant mutants of moss, *Physcomitrella patens*. *Mol Gen Genet* 154:87–95.

50. Naito H, Goshima G (2015) NACK kinesin is required for metaphase chromosome alignment and cytokinesis in the moss *Physcomitrella patens*. *Cell Struct Funct* 40:31–41.

51. Yasuhara H, Oe Y (2011) TMBP200, a XMAP215 homologue of tobacco BY-2 cells, has an essential role in plant mitosis. *Protoplasma* 248:493–502.

52. Van Damme D, et al. (2004) In vivo dynamics and differential microtubule-binding activities of MAP65 proteins. *Plant Physiol* 136:3956–3967.

53. Marc J, et al. (1998) A GFP-MAP4 reporter gene for visualizing cortical microtubule rearrangements in living epidermal cells. *Plant Cell* 10:1927–1940.

54. Murata T, Baskin TI (2014) Imaging the mitotic spindle by spinning disk microscopy in tobacco suspension cultured cells. *Methods Mol Biol* 1136:47–55.

55. Hiwatashi Y, et al. (2008) Kinesins are indispensable for interdigitation of phragmoplast microtubules in the moss *Physcomitrella patens*. *Plant Cell* 20:3094–3106.

Supporting Information

Kosetsu et al. 10.1073/pnas.1713925114
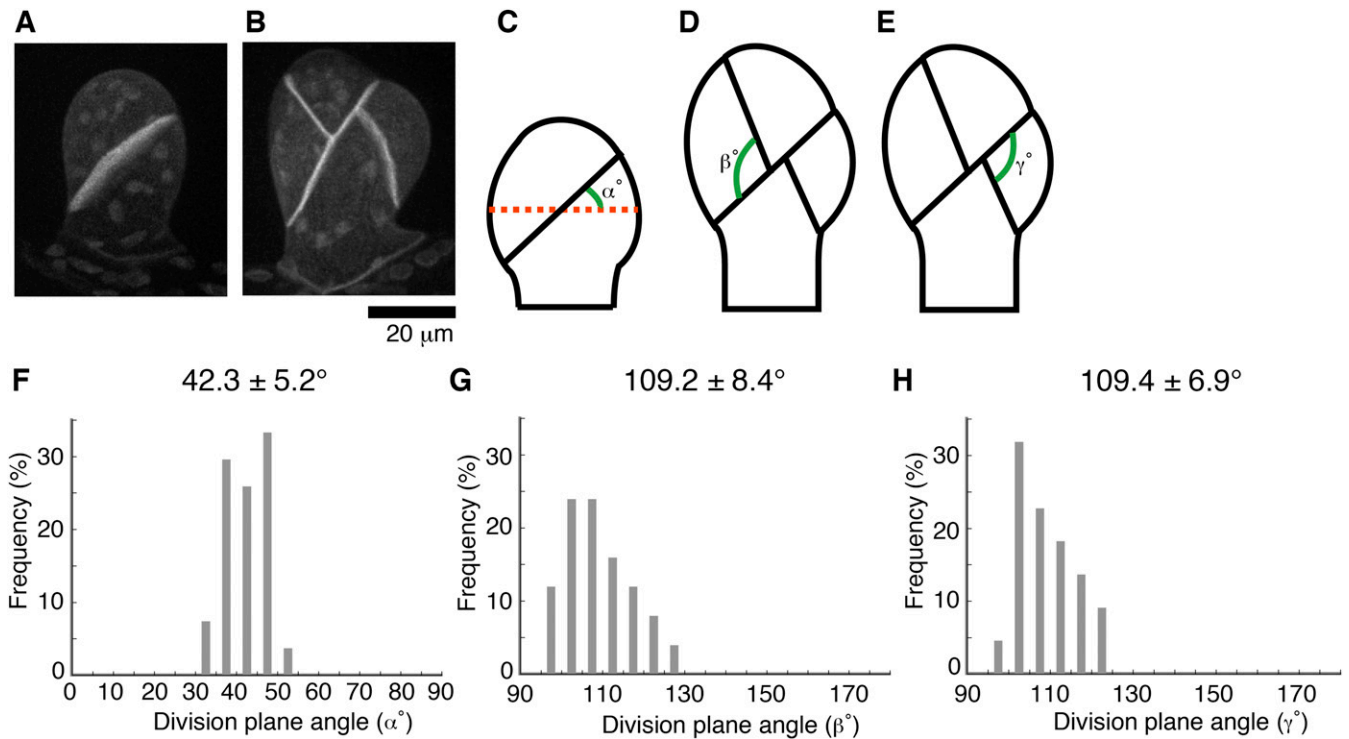
Fig. S1. The division plane orientation in the gametophore initial is tightly controlled. (*A* and *B*) Oriented cell plate formation at two- and four-cell stages of the gametophore initial. The cell membrane was visualized by Citrine-SYP1a. Images were acquired with 51 *z*-sections (separated by 1 μm) and displayed after maximum projection. (Scale bar, 20 μm.) (*C*–*H*) Schematic representation and quantification of division plane orientation in the first three divisions. The reference line (red dots) was set perpendicular to the growth direction (α) or to the division plane of the first division (β and γ). Mean values ± SD are displayed.
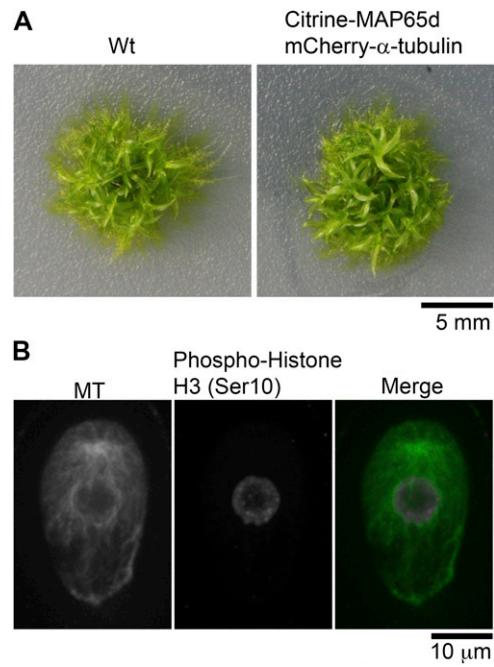
Fig. S2. Marker gene expression causes no morphological developmental differences of moss. (*A*) Gross morphology of wild-type and the transgenic moss expressing the mCherry–α-tubulin and Citrine-MAP65d (19-d-old plants). (*B*) Visualization of the endogenous MTs in the gametophore initial cell by immunostaining using anti–α-tubulin reveals the presence of the gametosome in wild-type moss. Anti-H3S10ph antibody staining was used to correlate gametosome appearance with the proper cell cycle phase. Images were acquired with 6 z-sections (separated by 1 μm), and displayed using maximum projection.
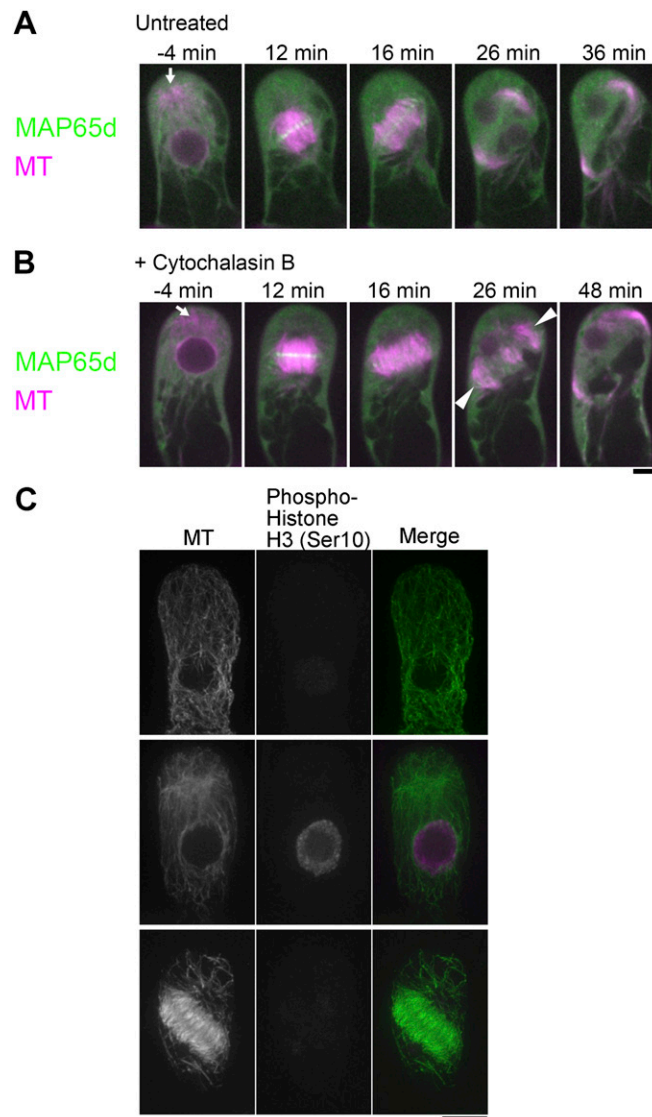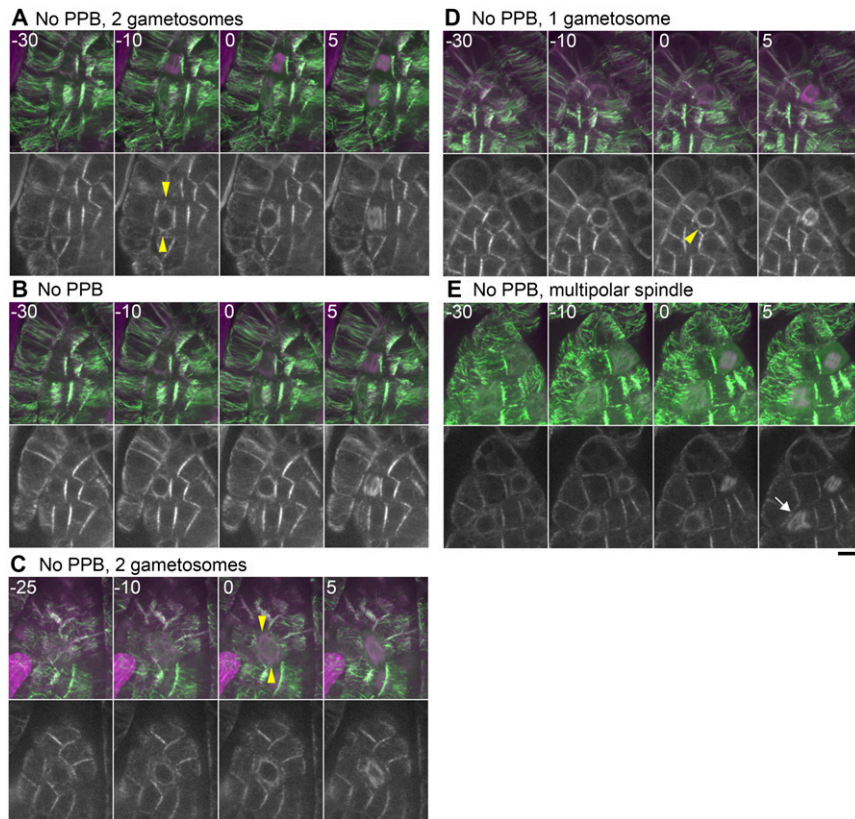
Fig. S3. F-actin and Myo8 are not required for gametosome formation. (*A* and *B*) Time-lapse imaging of mCherry–α-tubulin (magenta) and Citrine-MAP65d (green) during the first division of the gametophore initial cell with (*B*) or without (*C*) 200 μM Cytochalasin B, an actin inhibitor. Images were recorded every 2 min. Time 0 corresponds to the timing of NEBD. Arrowheads indicate loosened MT interdigitations, which lack prominent Citrine-MAP65d signals. Gametosomes are marked by arrows. (Scale bar, 10 μm.) (*C*) Immunostaining of endogenous MTs in the gametophore initial of the *myo8* null mutant confirmed the Myo8-independent formation of the gametosome. Images were acquired with six *z*-sections (separated by 1 μm), and displayed after maximum projection. (Scale bar, 10 μm.)

Fig. S4. Gametosome formation during cell division in leaf-like gametophore cells with detectable PPBs. (*A–H*) Time-lapse imaging of gametophore cells expressing Citrine-MAP65d (green) and mCherry–α-tubulin (magenta). Images were recorded every 5 min with 16 *z*-sections (separated by 1 μm), and displayed after maximum projection (*Top*, merged) or as single median slices (*Bottom*, grayscale). White and yellow arrowheads indicate the PPB and gametosome, respectively. Arrows indicate multipolar spindles. Time 0 corresponds to the timing of NEBD. (Scale bar, 10 μm.)

Fig. S5. Gametosome formation during cell division in leaf-like gametophore cells without clear PPBs. (*A–E*) Time-lapse imaging of Citrine-MAP65d (green) and mCherry–α-tubulin (magenta) in mature gametophore cells. Images were acquired every 5 min with 16 *z*-sections (separated by 1 μm) and displayed after maximum projection (*Top*, merged) or as single median slices (*Bottom*, grayscale). Time 0 corresponds to the timing of NEBD. White and yellow arrowheads indicate the PPB and gametosome structures, respectively. The arrow indicates a multipolar spindle. (Scale bar, 10 μm.)

Table S1. List of primers used in this study

Constructs	Sequences (5′ → 3′) (forward and reverse)
Citrine-SYP1a construct (left arm)	GGGGTACCAGCTCTAGCGCGTTGAATTG
	ACGCGGGCCCAGTGACTCACTCTCAAGCAA (Underline = Kpn1 site and Apa1 site)
Citrine-SYP1a construct (right arm)	GGACTAGTTATGAACAACCTTCTTAGCAACTCG
	TCCCCGCGGCAAGGGAACTCGCTATGCTT (Underline = Spe1 site and Sac2 site)
Citrine-MAP65d construct (left arm)	GGGGTACCTGAACGATTGTCGGAGTTGC
	CCCAAGCTTTGTGGCTTCTACAAGATCACC (Underline = Kpn1 site and Hind3 site)
Citrine-MAP65d construct (right arm)	GGACTAGTTATGGTTCAGCAGCCTGTGAC
	ATTTGCGGCCGCCCATACCGACCCACTTCGTA (Underline = Spe1 site and Not1 site)
TON1 KO construct (left arm)	GGGGTACCGATTGAGCCCTCTGCCAAAC
	CCATCGATGTAAAACGACTTCTTACAACCTTCA (Underline = Kpn1 site and Cla1 site)
TON1 KO construct (right arm)	CGGGATCCAAATTTGAAATTTCTCACCTTACGT
	ATTTGCGGCCGCGAGTTTCACGTCACCTAACCAG (Underline = BamH1 site and Not1 site)
Lifeact-GFP construct	CACCATGGGTGTCGCAGATTTGAT
	TTACTTGTACAGCTCGTC
mCherry/α-tubulin construct	CACCATGGTGAGCAAGGGCGAGGAG
	GCTCCTGCTCCTGCTCCGCTGTACAGCTCGTCCATGCCGC
mCherry/α-tubulin construct	AAAGCGGCCGCGGGCCCCACCATGGTGAGC
	TTTACTAGTACCTGCTCCTGCTCCTGCTCCTGCTCCTGCTCCGC (Underline = Not1 site and Spe1 site)
mCherry/α-tubulin construct	GGTACTAGTATGAGAGAGATTATC
	TATGGCGCGCCGGGCCCTCAGTAGTCGTCGTCCTCCG (Underline = Spe1 site and Asc1 site)
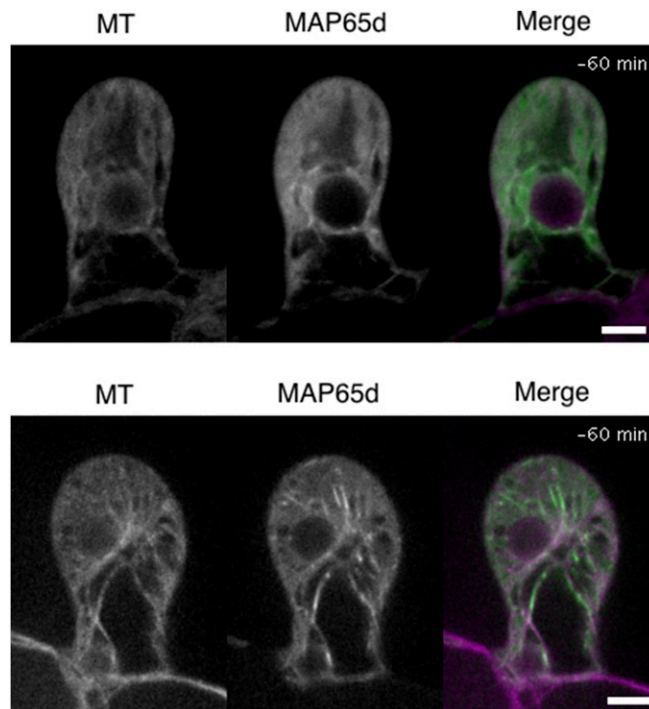
Movie S1. Time-lapse observation of Citrine-MAP65d and mCherry–α-tubulin during the first, second, and third divisions of the gametophore initial. (Scale bars, 10 μm.)
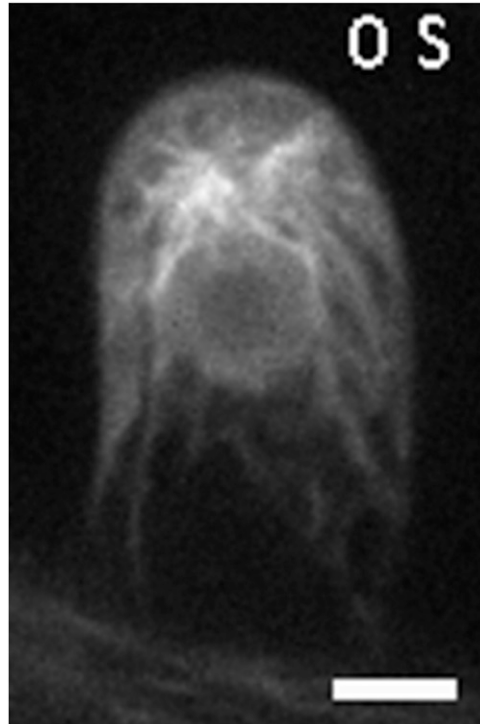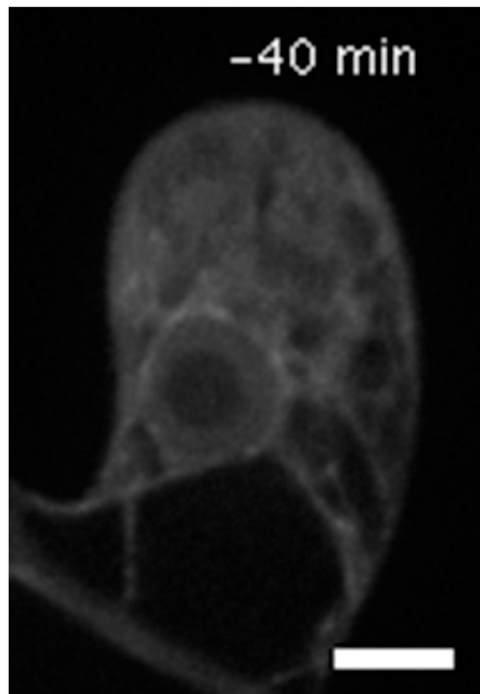
[Movie S1](#)

Movie S2. Time-lapse observation of mCherry–α-tubulin during the first division of the gametophore initial. (Scale bar, 10 μm.)
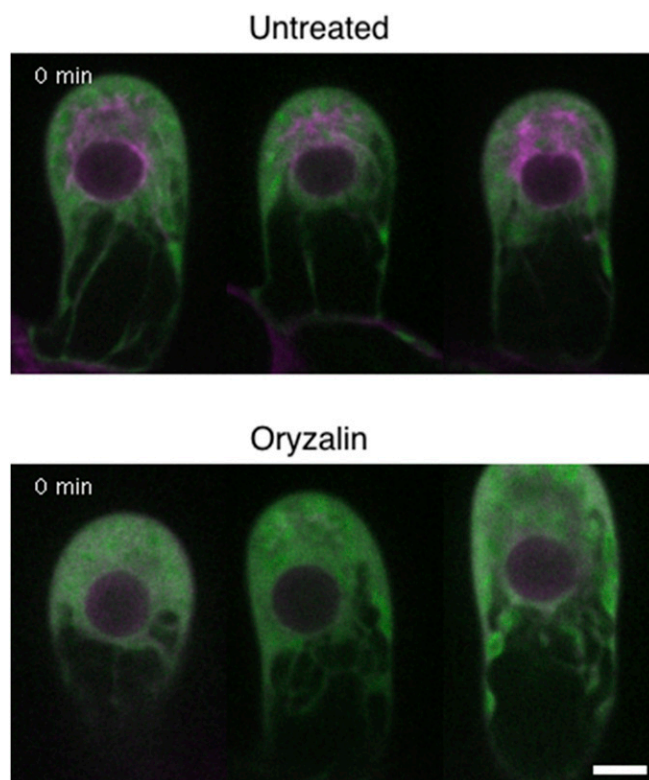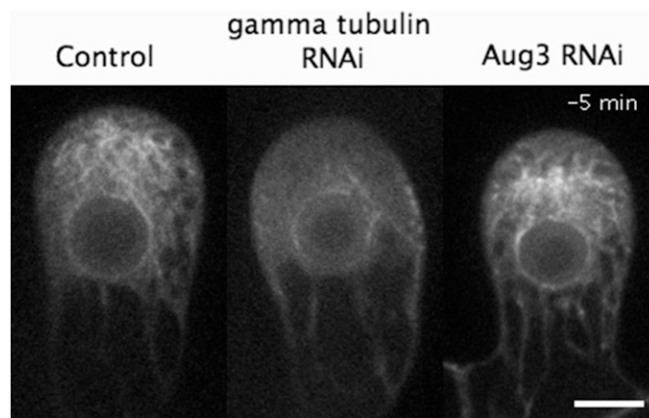
[Movie S2](#)

Movie S3.   Time-lapse observation of mCherry–α-tubulin in a cell transiently treated with oryzalin. (Scale bar, 10 μm.)

Movie S3

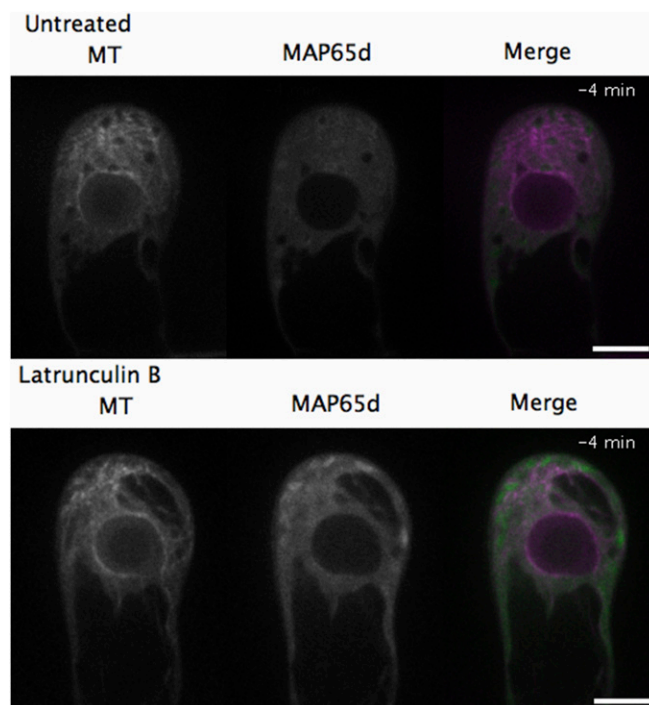
Movie S4.   Other examples of mitosis after transient treatment of oryzalin or control DMSO. mCherry–α-tubulin was imaged. (Scale bar, 10 μm.)

Movie S4

Movie S5. Time-lapse observation of mCherry–α-tubulin in control, the γ-tubulin. RNAi line and the Aug3 RNAi line showing that the latter two fail to produce a bipolar spindle. (Scale bar, 10 μm.)

Movie S5

Movie S6. Time-lapse observation of mCherry–α-tubulin and Citrine-MAP65d with or without latrunculin B. (Scale bars, 10 μm.)

Movie S6

Movie S7. Time-lapse observation of Citrine-MAP65d and mCherry–α-tubulin in leaf-like gametophore cells. *Left* (merged) shows maximum projections while *Right* (grayscale) shows single optical slices.The white arrowhead indicates the position of the PPB, and the yellow arrowheads indicate gametosomes. (Scale bars, 10 μm.)

Movie S7